SSRG International Journal of Mechanical Engineering
ISSN: 2348 – 8360 / https://doi.org/10.14445/23488360/IJME-V9I6P101

Volume 9 Issue 6, 1-7, June 2022

Original Article

Modelling and Finite Element-Based Analysis of Grasping of a Cuboidal Shaped Object by a Five Fingered Underactuated Robotic Hand

Deepak Ranjan Biswal[1], Dibyendu Sekhar Sahoo[2], Bikram Keshari Routray[3]

[1,2,3]*Department of Mechanical Engineering, DRIEMS (Autonomous) Odisha, India*

Received: 15 March 2022 Revised: 03 May 2022 Accepted: 18 May 2022 Published: 22 June 2022

Abstract - *In humanoid robotics, it is a great challenge to provide a robotic system with handy ability and autonomous skills, specifically in the field of Industrial manufacturing, Prosthesis, orthopedic rehabilitation, etc. A complex level of actuation and transmission system is required for a multi-fingered hand to perform its operation. The underactuated concepts come to be a possible solution to achieve robotic hands with high dexterity without complicated mechanical design. The major features of an underactuated robotic hand are that the number of required actuators to control the hand is less than its degree of freedom. The underactuation decreases the complexity of the control system impressively and is much less expensive than the fully actuated equivalent hand. The present work dealt with modelling and finite element-based investigation of a five-fingered Robotic hand used to grasp a cuboidal-shaped object; the hand comprises four underactuated fingers, a self-operated thumb, and a palm.*

Keywords *- Dexterous, Grasping, Prosthesis, Tendondriven, Underactuation.*

1. Introduction

The growing interest in robotic hand development increases due to the extensive range of applications such as pick and place tasks, upper limbs prosthesis, flexible mechanization of abundant manufacturing jobs, automatic assembly duties, and works in an unstructured environment. Current industrial advancements are limited to precise grippers and insufficient tools when the robot must deal with the dextrous grasping of varying geometrical shapes and size substances. To accomplish the above-challenged applications, accepting the design of the human hand looks to be an acceptable solution because the hand of the human is the utmost developed and diverse external end of the human body and a millennium advancement outcome.

The TUAT/Karlsruhe hand, developed in 2021, has 5 fingers and 20 degrees of freedom and is powered by a single actuator that can be placed inside or outside the hand [1]. The analysis of the material and design structure of a three-fingered robot hand is proposed by M. H. bin Mohamed Azri and R. L. A. Shauri. This work presents a finite element analysis method for examining the robot assembly established on the robot design and the materials used for robot components [2]. A review of anthropomorphic robotic hand developed in recent years are presented by G.Melo et al., 2014 [3]. S.S. Bhavikatti introduced Finite Element Analysis in 2005[4]. An overview of the finite element method is described [5]. Gosselin et al., 2008 recommended an anthropomorphic hand of an underactuated type having 15 dofs and one actuator. This project aims to look into the possibility of making a versatile hand out of a single actuator [6].

Smart hand a 16 Degrees of freedom and 4 Degrees of actuation underactuated anthropomorphic hand presented in 2010[7]. This hand has 5 fingers and 4 actuators, and all the actuators are inside the palm. The first actuator is responsible for the flexion/extension of the thumb, the second for flexion/extension of the index, the third for flexion/extension of the middle, ring, and little finger, and the fourth one is responsible for thumb abduction/adduction. Vincent's hand, developed in 2011, is a 6-DOF, 6-DOA viable prosthetic hand. This hand is alike a human hand having five fingers, i.e., 4 fingers and one thumb. It is a myoelectric-controlled hand. Except for the double-actuated thumb, it has a single actuator for thumb abduction/adduction drive and the other for thumb flexion. There are a total of 6 actuators in total [8]. Lee et al.,2017 proposed KITECH-Hand, an extremely agile and modularized robotic hand of an anthropomorphic type which is a fully actuated hand with a total of 16DOF [9]. A novel super underactuated multi-fingered TH-2 hand was designed in 2006 for a humanoid robot constructed on a preceding under-actuated finger mechanism[10]. TUAT/Karlsruhe hand, developed in 2021, has 5 fingers, 20

DOFs, and is powered by a single actuator that can be placed inside or outside the hand [11]. HIT/DLR hand is a prosthetic hand, a multi-sensory five-fingered bio-prosthetic hand Similar to the adult's hand. It has 13 joints, with three motors, each controlling the thumb, index finger, and the other three fingers. [12]. In 2016, RBO Hand-2, a novel type of highly biddable, underactuated, tough, and agile anthropomorphic hand, was proposed. The hand can perform 31 of the 33 grasp deportments of the human hand listed in the inclusive Feix taxonomy[13]. A Super under-actuated multi-fingered TH-3R hand is proposed, which is a self-adaptive one having gear and rack mechanism and spring constraints. This hand consists of similar fingers of 5 numbers with a whole of fifteen degrees of freedom. [14]. IH2 AZZURRA SERIES is an anthropomorphic underactuated hand with 5 fingers, i.e., 4 fingers and a thumb. This hand has self-adaptive fingers with manually adjustable stiffness that wrap around objects automatically. This hand is tendon-actuated with an adjustable Bowden cable transmission mechanism [15]. A highly underactuated ADAM hand comprises 5 fingers controlled by 1 actuator developed in 2017 for prosthesis purposes. The five fingers on this hand are connected to a fixed frame via revolute joints, similar to a human palm. The transmission mechanism is adaptive on this hand [16]. Konnaris et al. 2016 proposed a tendon-driven robot hand, which is actuated by seven motors and accomplishes rolling the object in hand [17]. A prosthetic hand with multiple functions was proposed by Gopura et al., 2020. This study proposes a MORA Hap-2 hand with self-adaptation capability. This hand allows the user to grasp various objects by performing cylindrical grasping, hook grasping, lateral pinching, tip pinching, and palmar pinching. [31]

In 2010, G. Mode and C. Hand proposed the COSA-DTS hand as a Unique Coupled and Self-adaptive Under-actuated one. The fingers of this hand grasp objects using a special COSA grasping mode, which includes two processes, i.e., a coupled grasping method and a self-adaptive grasping process.[19]. Accurate grasping and manipulation of small substances from flat surfaces using underactuated fingers were proposed by Odhner and Dollar [20]. Hussain et al., 2018 proposed analytical modelling of flexure joints based on screw theory[21]. Power grasp planning for anthropomorphic robot hands was proposed by Roa et al., 2012. The author presented a methodology for Bcalculating power grasps for hands with kinematic structures similar to the human hand, which permits the execution of plans motivated by human grasping schedules[32]. A. Bicchi and V. Kumar reviewed robotic grasping and the work done in this area over the last two decades, with a slight bias toward the progress of the theoretical outline and analytical results in this part [23]. An investigation of grasping an object, the progress of a theory of pushing in consideration of friction, and using these theories in the automatic planning of grasping tasks are presented [24].

A summary of the evolution and current state of the art in the subject of robot hands is presented. The survey focuses on three sorts of functional requirements that might be recognised by a machine hand in an artificial system [25]. Accurate and fast grasp is an important issue presented by the author [26]. An investigational methodology to fast precision grasp planning for arbitrarily shaped 3D objects is described by M. Buss et al., 1996 [27]. J. Huges et al., 2016 reviewed the grippers and Soft Manipulators. The author focuses on the existing materials and procedures, actuation methods, and sensors used to expand soft manipulators [28]. RBO Hand-2, a novel kind of amenable under-actuated anthropomorphic robotic hand for skillful grasping, is presented [13].

Because of this, the present work deals with modelling a hand with five fingers approximately the size of the human hand. The modelled robotic hand is underactuated in which individual motors make the flexion/extension motion of the four fingers, and individual motors make the abduction/adduction motion of the four fingers. So a total of 8 actuators are used for four fingers. The thumb comprises 5 motors for the motion. The underactuated robotic hand consists of 21 degrees of freedom with 13 motors. The modelled hand is designed to grasp a cuboid-shaped object. The various mechanical parameters are analysed in the Ansys platform.

Table 1. Lengths of the phalanges of the hand

Name	Length of Metacarpal bones	Length of Proximal Phalangeal bone	Length of Middle Phalangeal bone	Length of Distal Phalangeal bone
Thumb	$0.251 * L$	$0.196 * L$		$0.158 * L$
Index	$\sqrt{(0.374L)^2 + (0.126\overline{B})^2}$	$0.265 * L$	$0.143 * L$	$0.097 * L$
Middle	$0.373 * L$	$0.277 * L$	$0.170 * L$	$0.108 * L$
Ring	$\sqrt{(0.336L)^2 + (0.077\overline{B})^2}$	$0.259 * L$	$0.165 * L$	$0.107 * L$
Little	$\sqrt{(0.295L)^2 + (0.179\overline{B})^2}$	$0.206 * L$	$0.117 * L$	$0.093 * L$

2. Materials and Methods

The material used for the proposed hand model and grasping the objects are stainless steel, grey cast iron, and FR-4(Flame Retardant).FR-4 is a glass-reinforced epoxy laminate composite material. It consists of woven fiberglass cloth with a binder of epoxy resin resistant to flame. The detailed proposed hand dimensions are described in Table 1, which indicates the dimensions of different phalynx[30], where L and B are the length and width of the proposed robotic hand.

The detailed model of the proposed hand is presented in fig.1, in which all the phalanges and the joints are indicated with a number of degrees of freedom.

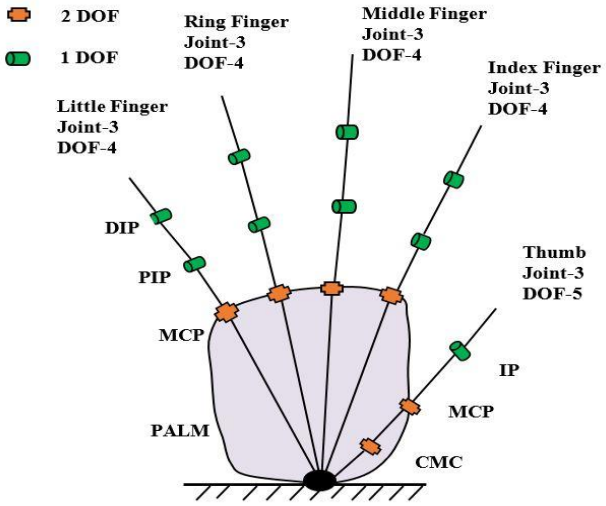

Fig. 1 Layout of the hand showing joints and Dof

The solid work model of the robotic hand is shown in fig.2, where all the fingers with the phalanges are modelled.

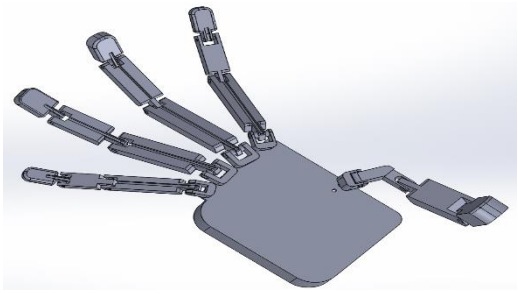

Fig. 2 Modelling of the hand

2.1. Grasping

In grasping, the desired object is held in place by the actions of the fingers of a hand. To grasp an object, the hand and individual fingers must be moved. There are two types of hand motion: free motion and restrained motion. Opening, Closing, and Clawing are three separate hand actions. A resisted motion is one in which the hand and fingers move against an external resistance. Power grip, Precision grip, and Pinch are three different resistive hand gestures. Various methods can accomplish grasping, and in the present paper, Tendon, the pulley mechanism is used to actuate the fingers.

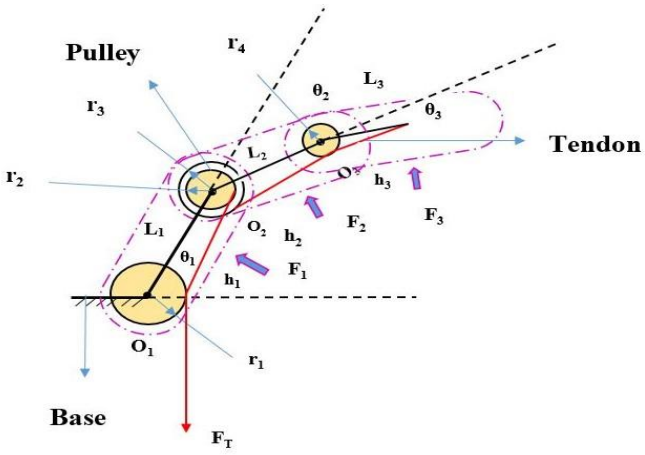

Fig. 3 Tendon Pulley arrangement of the hand

2.2. Contact Force Calculation

The schematic diagram of the tendon pulley arrangement with contact forces is shown in Fig.3. During the grasping process, forces will be formed at the contact points between the object and the three phalynx of a single finger. The normal contact force vector can be written as in eqn.1

$$f = [f_1 f_2 f_3]^T \tag{1}$$

F_1 is the proximal phalynx contact force, f_2 is the middle phalynx contact force, and f_3 is the distal phalynx contact force. The contact forces at the proximal phalynx, i.e., f_1, middle phalynx f_2, and distal phalynx f_3 are mentioned in equations 2, equation3 and equation 4 mentioned below

$$f_1 = \frac{KT_a}{h_1 h_2 h_3 r_1 r_3} \tag{2}$$

Where $K = A + B + C$

The values of *A*, *B*, and *C* are as follows

$$A = L_1 r_2 \cos\theta_2 \,(r_4 L_2 \cos\theta_3 + (r_4 - r_3)k_3)$$

$$B = -L_1 r_2 r_4 h_2 \cos(\theta_2 + \theta_3)$$

$$C = (r_1 - r_2) h_2 h_3 r_3$$

Middle and distal phalynx force is as follows.

$$f_2 = \frac{-r_2(-h_3 r_3 + r_4 L_2 \cos\theta_3 + r_4 h_3) T_a}{h_2 h_3 r_1 r_3} \tag{3}$$

$$f_3 = \frac{r_2 r_4 T_a}{h_3 r_1 r_3} \tag{4}$$

3. Results and Discussion

Calculating forces at the contact point at the three phalanges of the ring finger is taken here by considering the dimensions of the phalanges using the MATLAB Code. The length of the ring finger's proximal phalynx is approximately 47.92 mm. The lengths of the middle and the distal phalynx can be obtained from the formulation, as mentioned in table1.

3.1. Contact Force Graphs

The 3-dimensional graphs of the contact forces for the ring finger only are taken. The variation of contact forces f_1 with θ_2 and θ_3 is presented in Figure 4.

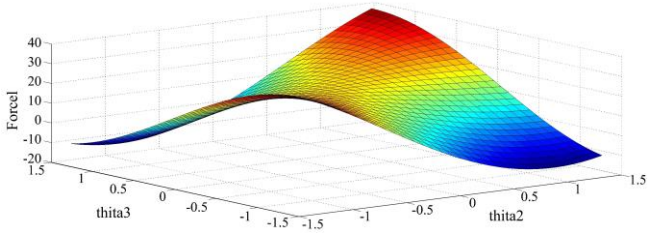

Fig. 4 Contact force f_1

The variation of contact force f_2 with angles θ_2 and θ_3 is presented in fig.5

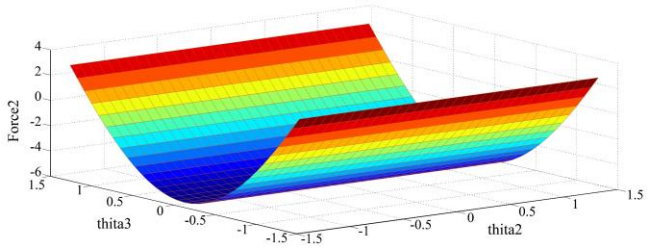

Fig. 5 Contact force f_2

The variation of contact force f_3 with angles θ_2 and θ_3 is presented in fig.6, which shows that the magnitude remains constant.

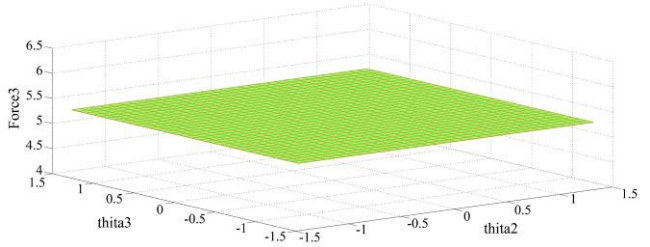

Fig. 6 Contact force f_3

3.2. Analysis of the Mechanical Properties

In the present article, the analysis of the modelled hand is presented. Three cases are taken into account, which are presented in this analysis. In case-A, the hand material comprising both the palm and the fingers is stainless steel, and the grasping object, i.e., the cuboid, is also stainless steel. In the case of B, the hand material is stainless steel, and the grasping object cuboid is grey cast iron. In case-C, the hand material is FR-4, and the cuboid is stainless steel. The Applied force varies from 10N to 100N vertically on the face of the cuboidal-shaped object. Various mechanical parameters were analysed in the Ansys-2021 environment. The mechanical properties analysed are Stress, Strain, and deformation. The modeling is done by solid work 2015, and the analysis is done. The target body taken in Ansys analysis is 5 touching distal phalanges total body of the fingers. The Contact body is the cuboid of dimensions (7.62 cm x7.62cm x7.62cm). Fixed support is all fingers and palms. Meshing details include the palm and fingers as triangular and the cuboid as square. All the phalanges, joints, and palms are fixed. Standard earth gravity g=9.81m/sec^2 is taken. Statistics in the Ansys workbench include that the total bodies are 36, active bodies are 36, total nodes are 40020, and total elements are 15546.

3.3. Analysis through Ansys

The total deformation at 50N force for case-A is analysed through the Ansys platform and is presented in fig.7.The stress and elastic strain at 50N force are mentioned below.

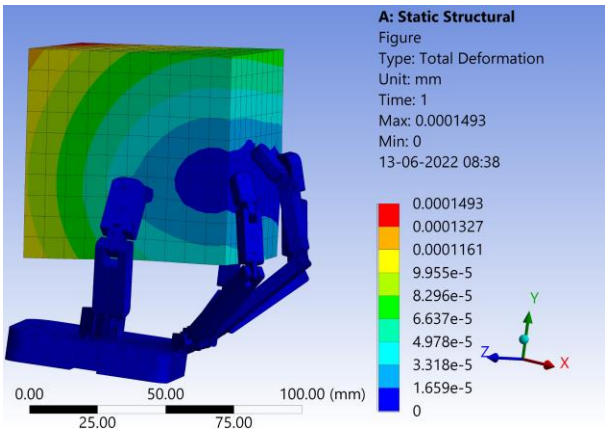

Fig. 7 Total deformation at 50N force

The equivalent stress analysis for case A is in fig.8.The maximum and the minimum values are mentioned in the analysis.

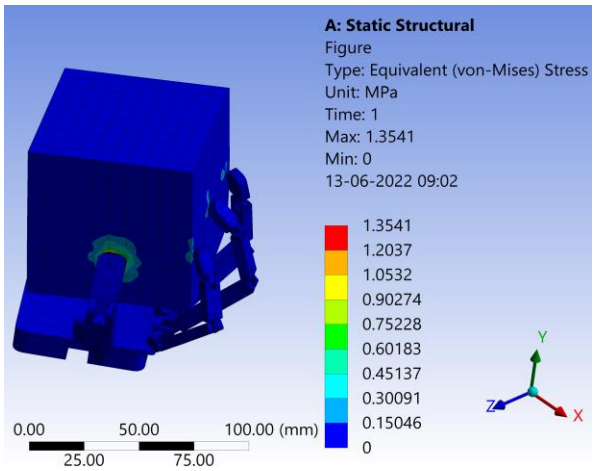

Fig. 8 Equivalent stress at 50N force

The equivalent strain analysis for case A is presented in fig.10.The analysis for case B and case C was also done in the Ansys platform, and the values are presented in the following table.

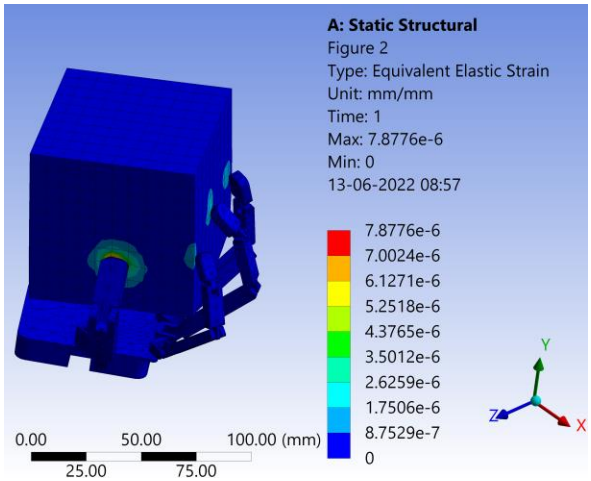

Fig. 9 Equivalent strain at 50N force

The values of all the mechanical parameters analysed for case-A are presented in table.2. The values of forces gradually increase from 10N to 100N. The maximum values at different values of force are presented.

The values of all the mechanical parameters analysed for case-B are presented in table.3. The values of forces gradually increase from 10N to 100N. The maximum values at different values of force are presented.

The values of all the mechanical parameters for case-C are presented in table.4. The values of forces gradually increase from 10N to 100N. The maximum values at different values of force are presented.

Table 2. Mechanical properties (case A)

Force (N)	Total Deformation (mm)	Equivalent Stress (Mpa)	Equivalent Elastic Strain (mm/mm)
10	7.25E-05	0.67649	3.91E-06
20	8.95E-05	0.83175	4.81E-06
30	1.07E-04	0.98701	5.70E-06
40	1.24E-04	1.1423	6.60E-06
50	1.49E-04	1.3541	7.87E-06
60	1.58E-04	1.4528	8.40E-06
70	1.75E-04	1.608	9.29E-06
80	1.92E-04	1.7633	1.02E-05
90	2.09E-04	1.9186	1.11E-05
100	2.26E-04	2.0738	1.20E-05

Table 3. Mechanical properties (case-B)

Force (N)	Total Deformation (mm)	Equivalent Stress (Mpa)	Equivalent Elastic Strain (mm/mm)
10	1.20E-04	0.64526	6.60E-06
20	1.50E-04	0.80191	8.20E-06
30	1.79E-04	0.95856	9.80E-06
40	2.09E-04	1.1152	1.14E-05
50	2.39E-04	1.2719	1.30E-05
60	2.68E-04	1.4285	1.46E-05
70	2.98E-04	1.5852	1.62E-05
80	3.28E-04	1.7418	1.78E-05
90	3.58E-04	1.8985	1.94E-05
100	3.87E-04	2.06	2.10E-05

Table 4. Mechanical properties (case-C)

Force (N)	Total Deformation (mm)	Equivalent Stress (Mpa)	Equivalent Elastic Strain (mm/mm)
10	7.75E-05	0.70897	4.12E-06
20	9.57E-05	0.87163	5.07E-06
30	1.14E-04	1.0343	6.02E-06
40	1.32E-04	1.197	6.96E-06
50	1.50E-04	1.3596	7.91E-06
60	1.68E-04	1.5223	8.86E-06
70	1.87E-04	1.685	9.80E-06
80	2.05E-04	1.8476	1.07E-05
90	2.23E-04	2.0103	1.17E-05
100	2.41E-04	2.173	1.26E-05

3.4. Comparison Graphs

The total deformation comparison between case-A, case-B, and case-C is shown in Figure 10. It shows that the deformation as per the load is a linear curve, and as the load increases, the total deformation is more in case B and least in case-A. For a particular load, the total deformation for case-A is more, and for case, B is the least.

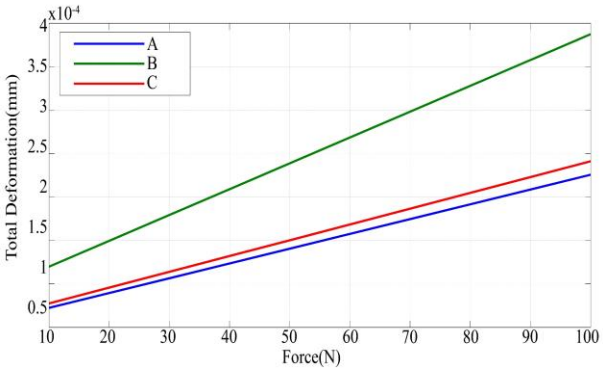

Fig. 10 Total deformation comparison

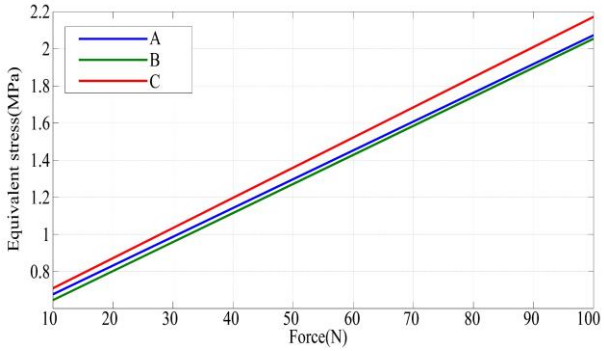

Fig. 11 Equivalent stress comparison

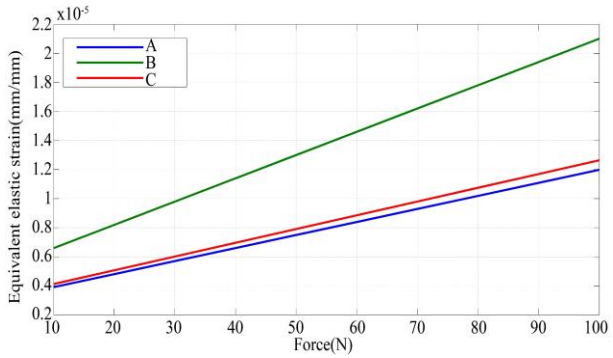

Fig. 12 Equivalent strain comparison

The equivalent stress comparison is shown in fig.11, which shows that the locus of the graphs is linear, and the equivalent stress is more in case C and least in case B as per the force increase. For a particular load, the Equivalent stress for case-C is more, and case-B is the least.

The Equivalent elastic strain comparison between all three cases is shown in Figure 12. The figure shows that the equivalent elastic strain per the force increase is a linear curve. As the load increases, the equivalent elastic strain is more in case B and least in case-A. The trajectory of the graphs is linear, and the maximum shear stress is more in case C and least in case B as per the force increase.

4. Conclusion

In this paper, modelling a robotic hand of underactuated type with five fingers is prepared through Solid work. The various parameters of the hand are studied and analysed in the ANSYS platform. The modelled hand grips the cuboid with all the fingers. The material is taken stainless steel as hand material, i.e., palm and fingers, and stainless steel for the cuboid in 1st case. In the 2nd case, the hand material is taken as stainless steel, and the cuboid is taken as stainless steel. In 3rd case, the hand material is taken as FR-4 material, and the palm material is grey cast iron. The various mechanical parameters are analysed, and the comparative graphs are presented.

References

[1] N. Fukaya et al., "Design of the TUAT/Karlsruhe Humanoid Hand," *Proceedings, IEEE/RSJ International Conference on Intelligent Robots and Systems*, vol. 3, pp. 1754-1759, 2000. [CrossRef] [Google Scholar] [Publisher Link]

[2] Muhammad Hafiz bin Mohamed Azri, and Ruhizan Liza Ahmad Shauri, "Finite Element Analysis of a Three-Fingered Robot Hand Design," *2014 IEEE 4th International Conference on System Engineering and Technology*, vol. 4, pp. 1-6, 2014. [CrossRef] [Google Scholar] [Publisher Link]

[3] E. N. Gama Melo, O. F. Aviles Sanchez, and D. Amaya Hurtado, "Anthropomorphic Robotic Hands: A Review," *Engineering and Development*, vol. 32, no. 2, pp. 279-313, 2014. [Google Scholar] [Publisher Link]

[4] S. S. Bhavikatti, *Finite Element Analysis*, New Age International, 2005. [Google Scholar] [Publisher Link]

[5] Vishal Jagota, Aman Preet Singh Sethi, and Khushmeet Kumar, "Finite Element Method: An Overview," *Walailak Journal of Science and Technology*, vol. 10, no. 1, pp. 1-8, 2013. [Google Scholar] [Publisher Link]

[6] Clement Gosselin, Frederic Pelletier, and Thierry Laliberte, "An Anthropomorphic Underactuated Robotic Hand with 15 Dofs and a Single Actuator," *2008 IEEE International Conference on Robotics and Automation*, pp. 749-754, 2008. [CrossRef] [Google Scholar] [Publisher Link]

[7] Christian Cipriani, Marco Controzzi, and Maria Chiara Carrozza, "Objectives, Criteria and Methods for the Design of the Smarthand Transradial Prosthesis," *Robotica*, vol. 28, no. 6, pp. 919-927, 2010. [CrossRef] [Google Scholar] [Publisher Link]

[8] Stefan Schulz, "First Experiences with the Vincent Hand," 2011. [Google Scholar] [Publisher Link]

[9] Dong-Hyuk Lee et al., "KITECH-Hand: A Highly Dexterous and Modularized Robotic Hand," *IEEE/ASME Transactions on Mechatronics*, vol. 22, no. 2, pp. 876-887, 2017. [CrossRef] [Google Scholar] [Publisher Link]

[10] Zhang Wen-zeng et al., "Superunderactuated Multifingered Hand for Humanoid Robot," *Frontiers of Mechanical Engineering in China*, vol. 1, no. 1, pp. 33-39, 2006. [CrossRef] [Google Scholar] [Publisher Link].

[11] T. Asfour, and R. D.-P. of the S. I. Symposium, Design of the TUAT/Karlsruhe Humanoid Hand, academia.edu, 2000. [Online]. Available: https://www.academia.edu/download/44186523/Design_of_the_TUATKarlsruhe_Humanoid_Han20160329-996-eo8lg.pdf

[12] Hai Huang et al., "The Mechanical Design and Experiments of HIT/DLR Prosthetic Hand," *IEEE International Conference on Robotics and Biomimetics*, pp. 896–901, 2006. [CrossRef] [Google Scholar] [Publisher Link]

[13] Raphael Deimel, and Oliver Brock, "A Novel Type of Compliant and Underactuated Robotic Hand for Dexterous Grasping," *The International Journal of Robotics Research*, vol. 35, no. 1-3, pp. 161–185, 2015. [CrossRef] [Google Scholar] [Publisher Link]

[14] Wenzeng Zhang et al., "Super Under-Actuated Multi-Fingered Mechanical Hand with Modular Self-Adaptive Gear-Rack Mechanism," *Industrial Robot*, vol. 36, no. 3, pp. 255-262, 2009. [CrossRef] [Google Scholar] [Publisher Link]

[15] Prensilia s.r.l., IH2 Azzurra series - Data Sheet, 2014. [Online]. Available: http://www.prensilia.com/files/support/doc/DS-IH2-v02.pdf

[16] Giovanni A. Zappatore, Giulio Reina, and Arcangelo Messina, "Analysis of a Highly Underactuated Robotic Hand," *International Journal of Mechanics and Control*, vol. 18, no. 2, pp. 17-24, 2017. [Google Scholar] [Publisher Link]

[17] Charalambos Konnaris et al., "EthoHand: A Dexterous Robotic Hand with Ball-Joint Thumb Enables Complex In-Hand Object Manipulation," *2016 6th IEEE International Conference on Biomedical Robotics and Biomechatronics*, pp. 1154-1159, 2016. [CrossRef] [Google Scholar] [Publisher Link]

[18] Hoang Thi Phuong, "Researching Robot Arm Control System Based on Computer Vision Application and Artificial Intelligence Technology," *SSRG International Journal of Computer Science and Engineering*, vol. 8, no. 1, pp. 24-29, 2021. [CrossRef] [Publisher Link]

[19] G. Mode and C. Hand, "A Novel Coupled and Self-adaptive Under-actuated Grasping Mode and the COSA-DTS Hand," *International Conference on Intelligent Robotics and Applications*, pp. 59-70, 2010. [CrossRef] [Google Scholar] [Publisher Link]

[20] Lael U. Odhner, Raymond R. Ma, and Aaron M. Dollar, "Precision Grasping and Manipulation of Small Objects from Flat Surfaces Using Underactuated Fingers," *2012 IEEE International Conference on Robotics and Automation*, pp. 2830-2835, 2012. [CrossRef] [Google Scholar] [Publisher Link]

[21] Irfan Hussain et al., "Modeling and Prototyping of an Underactuated Gripper Exploiting Joint Compliance and Modularity," IEEE Robotics and Automation Letters, vol. 3. no. 4, pp. 2854-2861, 2018. [CrossRef] [Google Scholar] [Publisher Link]

[22] Mohammed Farhan Jawad et al., "Farmer Robot for Harvesting and Maintaining Plants," *SSRG International Journal of Electrical and Electronics Engineering*, vol. 7, no. 1, pp. 7-11, 2020. [CrossRef] [Google Scholar] [Publisher Link]

[23] A. Bicchi, and V. Kumar, "Robotic Grasping and Contact: A Review," *Proceedings 2000 ICRA. Millennium Conference. IEEE International Conference on Robotics and Automation*, vol. 1, pp. 348–353, 2000. [CrossRef] [Google Scholar] [Publisher Link]

[24] M. T. Mason, and J. K. Salisbury Jr, *Robot Hands and the Mechanics of Manipulation*, 1985. [Google Scholar] [Publisher Link]

[25] A. Bicchi, "Hands for Dexterous Manipulation and Robust Grasping: A Difficult Road Toward Simplicity," *IEEE Transactions on Robotics and Automation*, vol. 16, no. 6, pp. 652-662, 2000. [CrossRef] [Google Scholar] [Publisher Link]

[26] C. Borst, M. Fischer, and G. Hirzinger, "A Fast and Robust Grasp Planner for Arbitrary 3D Objects," *Proceedings 1999 IEEE International Conference on Robotics and Automation*, vol. 3, pp. 1890-1896, 1999. [CrossRef] [Google Scholar] [Publisher Link]

[27] M. Buss, H. Hashimoto, and J. B. Moore, "Dextrous Hand Grasping Force Optimization," *IEEE Transactions on Robotics and Automation*, vol. 12, no. 3, pp. 406-418, 1996. [CrossRef] [Google Scholar] [Publisher Link]

[28] J. Hughes et al., "Soft Manipulators and Grippers: A Review," *Frontiers in Robotics and AI*, vol. 3, p. 69, 2016. [CrossRef] [Google Scholar] [Publisher Link]

[29] Maximo A. Roa et al., "Power Grasp Planning for Anthropomorphic Robot Hands," *2012 IEEE International Conference on Robotics and Automation*, pp. 563-569, 2012. [CrossRef] [Google Scholar] [Publisher Link].

[30] P. K. Parida, "*Kinematic Analysis of Multi-Fingered, Anthropomorphic Robotic Hands*," 2013. [Google Scholar] [Publisher Link]

[31] R. A. R. C. Gopura et al., 2020 6th International Conference on Control, Automation and Robotics, 2020.